RSC Advances

ROYAL SOCIETY OF CHEMISTRY

www.rsc.org/advances

Cite this: DOI: 10.1039/c0xx00000x

www.rsc.org/xxxxxx

ARTICLE TYPE

Simple and green synthesis of nitrogen-, sulfur-, and phosphorus-co-doped carbon dots with tunable luminescence properties and sensing application

Chunfeng Wang, Dong Sun, Kelei Zhuo*, Hucheng Zhang, Jianji Wang*

Received (in XXX, XXX) Xth XXXXXXXXX 20XX, Accepted Xth XXXXXXXXX 20XX
DOI: 10.1039/b000000x

A simple and green approach to prepare water-soluble, nitrogen-, sulfur-, and phosphorus-co-doped carbon dots (N/S/P-CDs) by one step hydrothermal treatment of cucumber juice is reported. The resultant N/S/P-CDs possess a uniform morphology, a size of less than 10 nm, plentiful O and N functional groups as well as the limited amount of P and S functional groups, and exhibit good luminescence stability, high resistance to photobleaching, high solubility, and excitation-independent emission behavior. It was also found that higher reaction temperature is in favor of the formation of N/S/P-CDs with smaller size and longer wavelength of photoluminescence emissions. Moreover, the N/S/P-CDs can be applied as a fluorescent probe for the detection of Hg^{2+} ion.

Introduction

Fluorescent carbon-based materials have attracted tremendous attention owing to their unique properties such as large two-photon absorption crosssection, high chemical inertness, facile functionalization, high resistance to photobleaching, low toxicity, and good biocompatibility.[1-3] The superior properties of these materials distinguish them from common toxic metal-based quantum dots, and make them promising alternatives for numerous exciting applications such as bioimaging,[4,5] drug delivery,[6,7] sensors,[3,8] and optoelectronic devices.[9-11] Fluorescent carbon-based materials primarily include carbon dots (CDs),[5,12] nanodiamonds,[13] carbon nano-tubes,[14] fullerene,[15] and fluorescent graphene.[4,16] Among all of these materials, CDs containing heteroatoms have generated especially a lot of excitement and been actively pursued, as they are considered the most promising candidate to complement carbon in materials applications because of their tunable intrinsic properties, such as electronic properties, surface and local chemical reactivities.[17,18] Therefore, great efforts have been made for the preparation of various types of CDs doped with heteroatoms. Currently, a broad series of methods for obtaining nitrogen-doped CDs have been developed,[3,19-21] but CDs doped with heteroatoms other than N, whether alone or with other dopants, have not been widely reported in the literature. Accordingly, it is still a great challenge to develop simple, green and efficient one-step strategies suitable for synthesizing heteroatom-co-doped CDs on a large scale.

Recently, there has been a trend to synthesize carbon-based materials from natural biomass, which are inexpensive, inexhaustible, and nontoxic, among other properties. Several successful demonstrations were given to prepare nanomaterials using biomass materials, which had many potential applications.[22-26] As we all know, cucumber abounds with carbon, nitrogen, oxygen, phosphorus, sulfur, and hydrogen elements owing to the existence of carbohydrate, protein, lipid, and glutathione. Thus, we expect this natural material to be a promising precursor for synthesizing heteroatom-co-doped CDs.

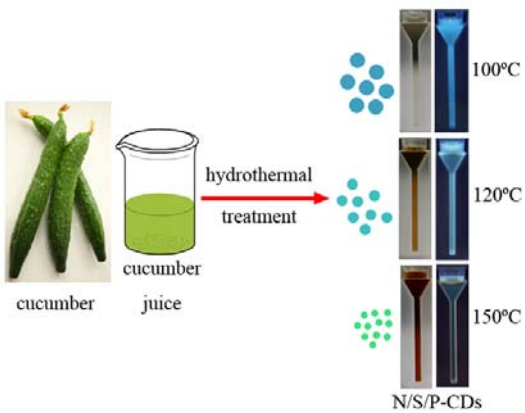

Fig. 1 Illustration of formation of N/S/P-CDs from hydrothermal treatment of cucumber juice. N/S/P-CDs: photographs were taken under visible light (left) and 365 nm UV light (right), respectively.

Herein, for the first time, we report on a simple, low cost, and green preparative strategy toward water-soluble, nitrogen-, sulfur-, and phosphorus-co-doped carbon dots (N/S/P-CDs) by one step hydrothermal treatment of cucumber juice, without any additives such as salts, acids or bases. Fig. 1 shows the synthesis procedure (see experimental section details). Our results show that the resultant N/S/P-CDs possess a uniform morphology, with a size of less than 10 nm, plentiful oxygen and nitrogen functional groups as well as the limited amount of phosphorus and sulphur functional groups, and excellent and stable fluorescent properties.

Moreover, the N/S/P-CDs can be applied as a fluorescent probe for the detection of Hg^{2+} ion.

Experimental Section

Materials and Apparatus

Cucumbers were purchased from local different supermarkets (The cucumbers were produced by different cultivation methods in different planting regions), and washed several times with water before use. $CaCl_2$, $Hg(NO_3)_2$, $MgCl_2$, $CuCl_2$, $Co(NO_3)_2$, $BaCl_2$, $CdCl_2$, $AgNO_3$, and $NiCl_2$ were purchased from Beijing Chemical Corp. $MnCl_2$, $Pb(NO_3)_2$, $FeCl_3$ and $AlCl_3$ were purchased from Tianjin Chemical Corp. All the chemicals were of analytical grade and used as received without further purication.

Ultraviolet-visible (UV-Vis) absorption spectra were obtained using a TU-1900 UV-vis Spectrophotometer (Beijing Purkinje). Fourier transform infrared (FTIR) spectra were recorded on a Nicolet 6700 spectrophotometer (Nicolet) using KBr pressed disks. The X-ray photoelectron spectra (XPS) measurements were performed on a Thermo Scientific K-Alpha electron energy spectrometer using Al Ka (1486.6 eV) as the X-ray excitation source. X-ray diffraction (XRD) measurements were performed on a Bruker D8 using Cu $K\alpha_1$ (1.54056 Å) as the incident radiation. High-resolution transmission electron microscopy (HRTEM) images were taken using a JEOL 2010 electron microscope at an accelerating voltage of 200 kV. The photoluminescence (PL) spectra were obtained using a FLS 980 fluorometer (Edinburgh Instruments Ltd.). Fluorescence lifetime and PL quantum yield (QY) measurements were carried on a FLS 980 fluorometer (Edinburgh Instruments Ltd.) equipped with an integrating sphere. The Integrating Sphere (IS) consists of a 120 mm inside diameter spherical cavity.

Synthesis of N/S/P-CDs

The cucumbers were squeezed at authors' laboratory with a juicing machine. The cucumber juices squeezed by using different cucumbers were uniformly mixed and filtrated with a 0.45 μm and 0.22 μm microporous membrane before use, respectively. N/S/P-CDs were synthesized by hydrothermal treatment of cucumber juice. In a typical procedure, 75 mL cucumber juice was transferred into a 100 mL Teflon-lined autoclave and heated at a constant temperature of 100 °C, 120 °C, or 150 °C for 6 h. The suspension was filtered through a 0.22 μm microporous membrane to remove the large dots, yielding yellow, brown, and brownish red N/S/P-CDs dispersion, respectively.

Fluorescence detection of Hg^{2+}

The detection of Hg^{2+} was performed at room temperature in phosphate buffer solution (PBS, 10 mM, pH 7.0). In a typical assay, 10 μL of N/S/P-CDs dispersion was added into 1 mL of PBS, followed by the addition of a calculated amount of Hg^{2+}. The PL emission spectra were recorded after reaction for 15 min at room temperature.

Results and Discussion

Characterization

XPS was used to analyze the chemical compositions and structures of the as-prepared N/S/P-CDs. Fig. 2a shows the existence of sulfur (around 164.0 eV), phosphorus (around 130.3 eV), carbon (around 285.0 eV), nitrogen (around 398.5 eV), and oxygen (around 531 eV) atoms. The content of each element is shown in Table 1. In detail, the spectrum of C_{1s} in the N/S/P-CDs (Fig. 2b) is deconvoluted into six single peaks at 284.5 eV, 285.3 eV, 286 eV, 286.5, 288.2 eV and 292.0 eV, which are attributed to C–C/C=C, C–S, C–N, C–O (epoxy and alkoxy), C=O, and π–π* satellite peak, respectively.[27,28] The N_{1s} spectrum has two peaks at 398.2 and 399.9 eV, which are attributed to the pyridinic N and pyrrolic N, respectively (Fig. 2c).[29] The O_{1s} spectrum is deconvoluted into two peaks at 531.6 and 533.1 eV (Fig. 2d), which can be assigned to P=O and P–O functional groups, respectively.[30] The S_{2p} spectrum (Fig. S1a, Supporting Information) is fitted into two peaks at 163.9 and 165.1 eV, which agree with the reported $2p_{3/2}$ and $2p_{1/2}$ positions of the –C–S– covalent bond of the thiophene-S, owing to their spin–orbit couplings.[31] The P_{2p} spectrum (Fig. S1b) is deconvoluted into two distinct components at 130.1 and 131.4 eV, which are attributed to $2p_{3/2}$ and $2p_{1/2}$, respectively.[30]

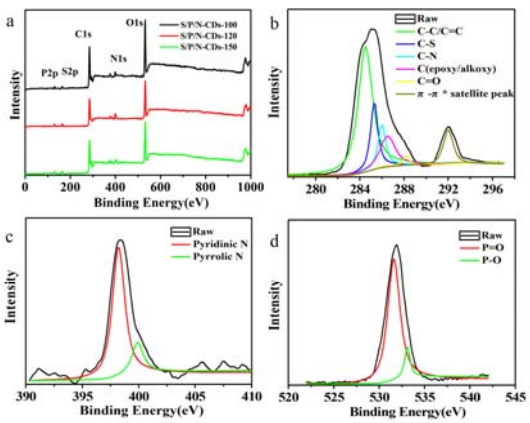

Fig. 2 (a) XPS spectra of different samples of N/S/P-CDs. (b–d) High-resolution XPS spectra of C_{1s}, N_{1s}, and O_{1s} of N/S/P-CDs.

Table 1 Elemental compositions of N/S/P-CDs prepared at different temperatures.

sample	C/atom%	N/atom%	S/atom%	P/atom%
N/S/P-CDs-100	62.79	4.27	0.19	0.22
N/S/P-CDs-120	63.14	4.04	0.21	0.24
N/S/P-CDs 150	63.89	3.83	0.24	0.28

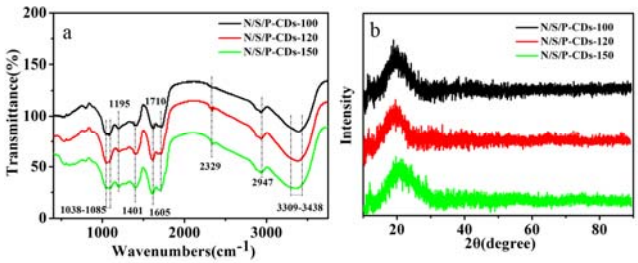

Fig. 3 FTIR spectra and XRD pattern of N/S/P-CDs.

Chemical and structural information about the N/S/P-CDs was

further obtained from the FTIR spectra. Fig. 3a shows the FTIR spectrum of N/S/P-CDs. The band at 1038~1085 cm^{-1} is assigned to the C–O–C, C–O, and P–O–C groups.[32,33] The peak at 1195 cm^{-1} is ascribed to the C–O, C–N, and C–S bonds.[23] The peak at 1401 cm^{-1} is identified as COO^- bonds.[34] Peaks at 1605 and 1710 cm^{-1} correspond to C=C stretching vibration[3] and C=O stretching vibration, respectively. The broad band at 3309–3438 cm^{-1} appears because of O–H and N–H bonds.[35] The peak at 2329 cm^{-1} is attributed to C–N and S–H bonds. The peak at 2947 cm^{-1} is the C–H bonds. Fig. 3b represents typical XRD profiles of N/S/P-CDs. XRD patterns of three kinds of N/S/P-CDs all displayed broad reflection center at *ca.* 19.5°, indicating that the (002) interlayer spacing distance of N/S/P-CDs is *ca.* 0.44 nm (Fig. S3). This value is larger than that of graphite (0.34 nm), possibly owing to the existence of oxygen-containing functional groups.[36,37]

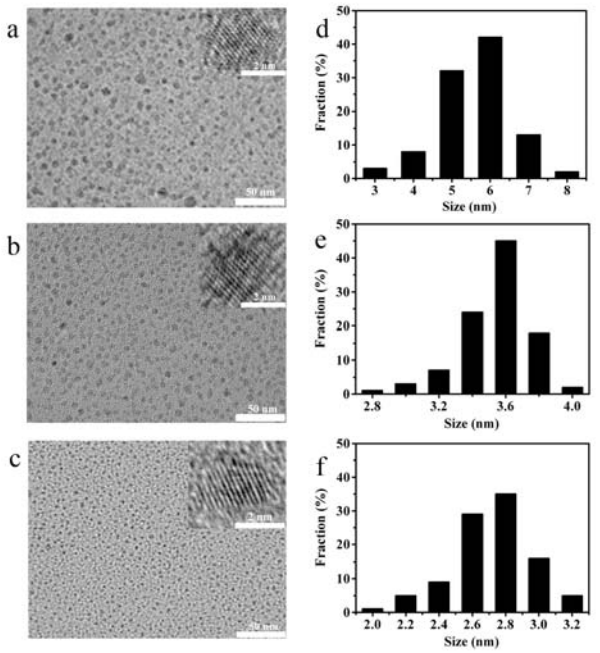

Fig. 4 Morphologies of the N/S/P-CDs. (a–c) TEM images of N/S/P-CDs-100, N/S/P-CDs-120, and N/S/P-CDs-150; Inset images are magnification of a single nanoparticle. (d–f) The particle size distribution histograms of N/S/P-CDs-100, N/S/P-CDs-120, and N/S/P-CDs-150.

TEM images (Figs. 4a-c) show that three kinds of N/S/P-CDs are uniform in size and well dispersed. The statistical particle size distributions of N/S/P-CDs-100 (Fig. 4d), N/S/P-CDs-120 (Fig. 4e) and N/S/P-CDs-150 (Fig. 4f) are mainly in the range of 3.0–8.0, 2.8–4.0 and 2.2–3.2 nm and have an average diameter of 5.6, 3.5 and 2.7 nm, respectively (100 random nanoparticles were accounted for each of three kinds of N/S/P-CDs). It is found that a higher reaction temperature gives a slightly smaller particle size and a relatively narrower size distribution. The high-resolution TEM (HRTEM) images (the inset images of Figs. 4a-c) show that three N/S/P-CDs samples (N/S/P-CDs-100, N/S/P-CDs-120 and N/S/P-CDs-150) possess the crystalline structure with lattice spacing of 0.20-0.22 nm, which are very close to the (100) diffraction planes of graphite.[38] This result indicates that the as-prepared N/S/P-CDs possess a graphite-like structure.

Optical Properties

To further explore the optical properties of the N/S/P-CDs, PL and UV–Vis absorption spectra were studied at room temperature. Figs. 5a-c reveal the UV–Vis absorption spectra of N/S/P-CDs synthesized at 100, 120, and 150 °C, respectively. A prominent red-shift from 257 to 283 nm is observed when the reaction temperature increases. The results revealed that the reaction temperature can affect the absorption properties of the as-synthesized N/S/P-CDs and that higher temperature leads to N/S/P-CDs absorption at longer wavelength. In fluorescence spectra, the N/S/P-CDs-100 has optimal excitation and emission wavelengths at 370 nm and 450 nm, respectively (Fig. 5d). When the reaction temperature increases, the excitation and emission wavelengths of N/S/P-CDs red-shift to: 418 nm and 505 nm for the N/S/P-CDs-120 (Fig. 5e); 514 nm and 571 nm for N/S/P-CDs-150 (Fig. 5f), respectively. The results show that the increase of reaction temperature can also lead to the redshift of the maximum excitation and emission wavelengths. The insets of Figs. 5d-f show the optical images of three N/S/P-CDs samples under UV light (365 nm) excitation. The N/S/P-CDs synthesized at temperatures of 100, 120, and 150 °C emit blue, greenish-blue, and green colors, respectively. The result reveals that the temperature can change the distribution of emission wavelength of the as-synthesized N/S/P-CDs. Different emission color may originate from different size, shape and defects of N/S/P-CDs.[39] TEM characterization (typical TEM images and size distribution for the N/S/P-CDs, see Fig. 4) also supports the conclusion that different-sized N/S/P-CDs yield different emission colors. The colors of three samples under daylight also become gradually deeper with increasing reaction temperature (see insets in Figs. 5a-c), which is consistent with previously reported results on carbon nanoparticles derived from candle soot and graphite.[40,41]

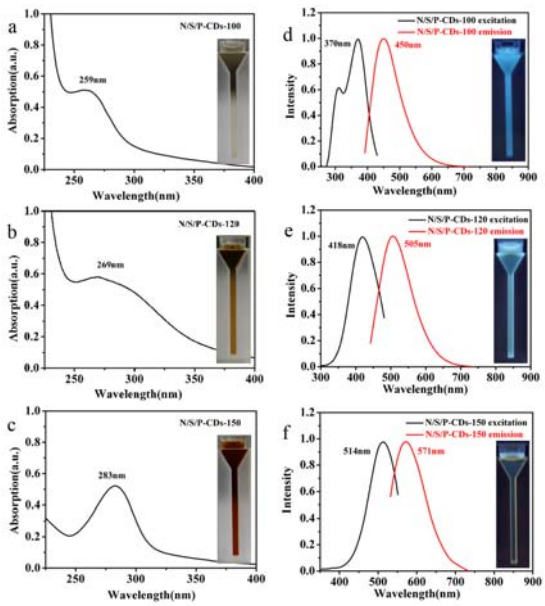

Fig. 5 The optical properties of (a and d) N/S/P-CDs-100, (b and e) N/S/P-CDs-120 and (c and f) N/S/P-CDs-150 aqueous solutions. (a, b, c) UV–Vis absorption spectra (inset: photographs taken under visible light). (d, e, f) Optimal excitation and emission PL spectra (inset: photographs taken under 365 nm UV light).

Excitation-dependent PL behaviors are a common

phenomenon observed in carbon fluorescent materials.[5,15,42–44] Similar to previous reports,[45,46] the as-prepared N/S/P-CDs also exhibited an excitation-dependent PL behavior. With the excitation wavelength change from 370 to 480 nm, the corresponding PL emission peak shifts from 450 to 540 nm for the N/S/P-CDs-100 (Fig. 6a). At the same time, the intensity of emission peaks becomes weaker. Both N/S/P-CDs-120 (Fig. 6b) and N/S/P-CDs-150 (Fig. 6c) are similar to the N/S/P-CDs-100.

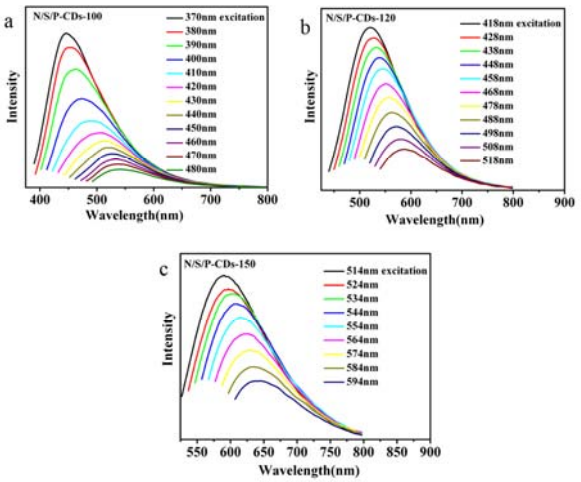

Fig. 6 The excitation-dependent PL behaviors of (a) N/S/P-CDs-100, (b) N/S/P-CDs-120, and (c) N/S/P-CDs-150.

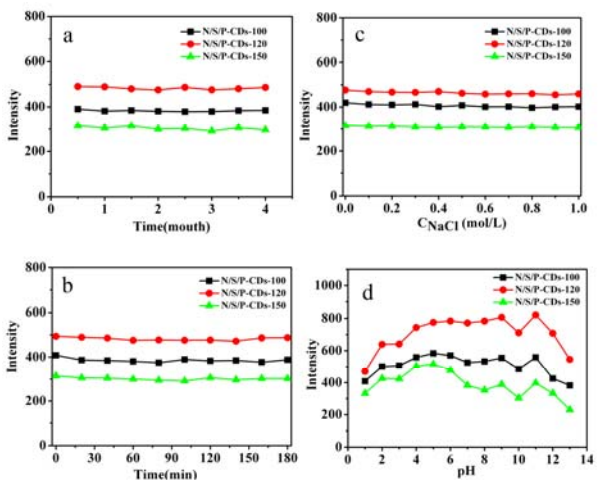

Fig. 7 Stability of N/S/P-CDs. (a) Effects of storage time on the fluorescence intensity of the N/S/P-CDs. (b) Effect of time intervals of irradiation with a UV lamp on fluorescence intensity of N/S/P-CDs. (c) Effect of ionic strengths on the fluorescence intensity of N/S/P-CDs (ionic strengths were controlled by various concentrations of NaCl in aqueous solution). (d) Effect of pH on the fluorescence intensity of N/S/P-CDs.

We further investigated their fluorescent properties under different conditions. First, as shown in Fig. 7a, their luminescence properties and appearance are nearly constant after the samples were stored for four months in air at room temperature. Second, their fluorescence intensities remain unchanged under UV irradiation for 3 h, indicating that the N/S/P-CDs are highly resistant to photobleaching (Fig. 7b). Third, their fluorescence intensities are almost unchanged with increasing concentrations of NaCl in aqueous solution (up to 1000 mM), showing high stability of the N/S/P-CDs even under the high ionic-strength conditions (Fig. 7c). Fourth, we investigated the fluorescence response of N/S/P-CDs at different pH values. It was observed that fluorescence intensities of N/S/P-CDs were not depended irregularly on pH values ranging from 1 to 13 (Fig. 7d), which agrees with the result reported in the literature.[2]

The QY of the CDs varies with the fabrication methods and the surface chemistry involved.[47] For the N/S/P-CDs, the highest QY (N/S/P-CDs-120) was measured to be 3.25% (Table S1), comparable to those of the reported luminescent carbon nanodots.[25,40,48,49] The luminescence decay profiles of the N/S/P-CDs are shown in Fig. S2. The decay was recorded with excitation and emission wavelengths of 404 nm and 481 nm for the N/S/P-CDs-100, 404 nm and 511 nm for the N/S/P-CDs-120, and 470 nm and 571 nm for the N/S/P-CDs-150 at room temperature using a time-correlated single photon counting technique. The fluorescence lifetime data for N/S/P-CDs were well fitted to a multi-exponential function (see Fig. S2). Fig. S2 lists the parameters generated from iterative reconvolution of the decay using the instrument response function (IRF) for all three samples. The average fluorescence lifetimes for different samples were calculated and listed in Table S1.

Fluorescence detection of Hg^{2+}

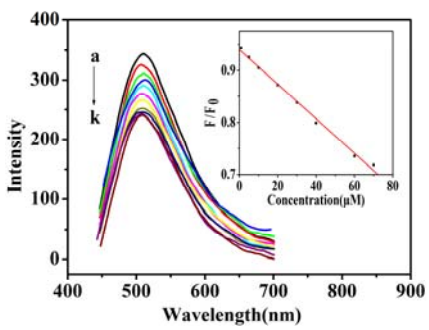

Fig. 8 The fluorescence responses of the N/S/P-CDs-120 in PBS (10 mM, pH 7.0) after the addition of different concentrations of Hg^{2+} (a to k): 0, 1, 5, 10, 20, 30, 40, 60, 70, 90 and 100 μM. The inset shows plot of the F/F_0 with the concentration of Hg^{2+}.

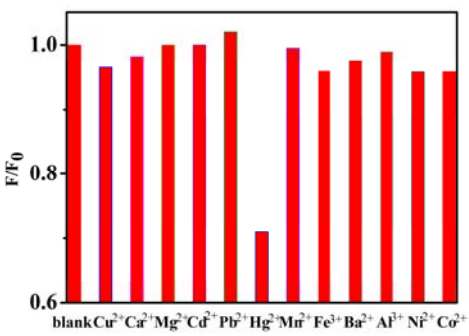

Fig. 9 F/F_0 of the N/S/P-CDs-120 in PBS (10 mM, pH 7.0) with 70 μM different metal ions. F and F_0 correspond to the fluorescence intensities of the N/S/P-CDs-120 with and without 70 mM of different metal ions, respectively.

Since the oxygen functional groups on the surface of N/S/P-CDs can interact with metal ions to form complex compounds by coordination, the N/S/P-CDs provide a potential possibility to be used as a fluorescent probe for the detection of metal ions.

Therefore, we explored the feasibility of the N/S/P-CDs-120 as a probe for the detection of Hg^{2+} in aqueous solutions. The results show that the strong emission of N/S/P-CDs-120 was quenched obviously when Hg^{2+} was added into the solutions, and the relative PL intensity (F/F_0, F and F_0 are the PL intensities of N/S/P-CDs-120 at 505 nm in the presence and absence of Hg^{2+} ion) of the N/S/P-CDs-120 is linear to the Hg^{2+} concentration in the range of 1–70 μM with a linear equation: $F/F_0 = -0.00332c + 0.940$ ($R = 0.9974$) (Fig. 8). The detection limit was 1.8×10^{-7} M. Furthermore, we investigated the fluorescence quenching effect of various metal ions on the N/S/P-CDs-120 as a probe (Fig. 9). It is seen that a much lower PL was observed for N/S/P-CDs-120 upon addition of Hg^{2+}. In contrast, no tremendous changes were observed upon addition of other ions into the N/S/P-CDs-120 dispersion. The outstanding selectivity can be probably attributed to the fact that Hg^{2+} has a stronger affinity toward the carboxylic group on N/S/P-CDs surface than other metal ions.[50,51]

To test the practicality of the developed method, we extended it to determine the concentration of Hg^{2+} in environmental water samples from the Weihe River in Xinxiang City. The fluorescence intensity of the N/S/P-CDs-120 decreased when the water samples were spiked with standard solutions. The recoveries of Hg^{2+} in the spiked samples were in the range of 101.0–102.4% (Table S2), illustrating little interference of the minerals, organics, and bacteria present in the samples. These results indicated the potential promise of the photoluminescent N/S/P-CDs in the practical applications.

Conclusion

In conclusion, we developed a simple, low cost, and green approach to prepare water-soluble, nitrogen-, sulfur-, and phosphorus-co-doped carbon dots by one step hydrothermal treatment of cucumber juice. The results showed that a higher reaction temperature is in favor of the formation of the N/S/P-CDs with smaller size, and longer wavelength of photoluminescence emissions. The obtained N/S/P-CDs exhibited good luminescence stability, high resistance to photobleaching, high solubility, and excitation-dependent emission behavior. Moreover, the material could be used as an effective fluorescent probe for the detection of Hg^{2+} ion with good selectivity and wide linear range in aqueous solution. We believe that the developed approach potentially opens up a simple and environment-friendly route to prepare heteroatom-co-doped CDs with broad application prospects.

Acknowledgments

Financial supports from the National Natural Science Foundation of China (No. 20973055, 21173070) and the Plan for Scientific Innovation Talent of Henan Province (No. 124200510014) are gratefully acknowledged.

Notes and references

Collaborative Innovation Center of Henan Province for Green Manufacturing of Fine Chemicals, Key Laboratory of Green Chemical Media and Reactions, Ministry of Education, School of Chemistry and Chemical Engineering, Henan Normal University, Xinxiang, Henan 453007, P. R. China. E-mail: klzhuo@263.net; Fax: +86-373-3329056; Tel: +86-373-3329056

† Electronic Supplementary Information (ESI) available: Fig. S1, Fig. S1, Table S1 and Table S2. See DOI: 10.1039/b000000x/

1 Y. P. Sun, B. Zhou, Y. Lin, W. Wang, K. A. S. Fernando, P. Pathak, M. J. Meziani, B. A. Harruff, X. Wang, H. F. Wang, P. J. G. Luo, H. Yang, M. E. Kose, B. L. Chen, L. M. Veca and S.Y. Xie, *J. Am. Chem. Soc.*, 2006, **128**, 7756.
2 D. Sun, R. Ban, P. H. Zhang, G. H. Wu, J. R. Zhang and J. J. Zhu, *Carbon*, 2013, **64**, 424.
3 S. J. Zhu, Q. N. Meng, L. Wang, J. H. Zhang, Y. B. Song, H. Jin, K. Zhang, H. C. Sun, H. Y. Wang and B. Yang, *Angew. Chem. Int. Ed.*, 2013, **52**, 3953.
4 S. J. Zhu, S. J. Tang, J. H. Zhang and B. Yang, *Chem. Commun.*, 2012, **48**, 4527.
5 Y. X. Fang, S. J. Guo, D. Li, C. Z. Zhu, W. Ren, S. J. Dong and E. K. Wang, *ACS Nano*, 2012, **6**, 400.
6 J. Tang, B. Kong, H. Wu, M. Xu, Y. C. Wang, Y. L. Wang, D. Y. Zhao and G. F. Zhang, *Adv. Mater.*, 2013, **25**, 6569.
7 Q. L. Wang, X. X. Huang, Y. J. Long, X. L. Wang, H. J. Zhang, R. Zhu, L. P. Liang, P. Teng and H. Z. Zheng, *Carbon*, 2013, **59**, 192.
8 F. Y. Yan, Y. Zou, M. Wang, X. L. Mu, N. Yang and L. Chen, *Sens. Actuators B*, 2014, **192**, 488.
9 V. Gupta, N. Chaudhary, R. Srivastava, G. D. Sharma, R. Bhardwaj and S. Chand, *J. Am. Chem. Soc.*, 2011, **133**, 9960.
10 X. Yan, X. Cui and L. S. Li, *J. Am. Chem. Soc.*, 2010, **132**, 5944.
11 H. T. Li, Z. H. Kang, Y. Liu and S. T. Lee, *J. Mater. Chem.*, 2012, **22**, 24230.
12 B. Kong, A. W. Zhu, C. Q. Ding, X. M. Zhao, B. Li and Y. Tian, *Adv. Mater.*, 2012, **24**, 5844.
13 A. Krueger, *Adv. Mater.*, 2008, **20**, 2445.
14 K. Welsher, Z. Liu, S. P. Sherlock, J. T. Robinson, Z. Chen, D. Daranciang and H. Dai, *Nat. Nanotechnol.*, 2009, **4**, 773.
15 J. Jeong, M. Cho, Y. T. Lim, N. W. Song and B. H. Chung, *Angew. Chem. Int. Ed.*, 2009, **48**, 5296.
16 S. J. Zhuo, M. W. Shao and S. T. Lee, *ACS Nano*, 2012, **6**, 1059.
17 O. Stephan, P. M. Ajayan, C. Colliex, P. Redlich, J. M. Lambet, P. Bernier and P. Lefin, *Science*, 1994, **266**, 1683.
18 A. B. Bourlinos, A. Bakandritsos, A. Kouloumpis, D. Gournis, M. Krysmann, E. P. Giannelis, K. Polakova, K. Safarova, K. Hola and R. Zboril, *J. Mater. Chem.*, 2012, **22**, 23327.
19 A. D. Zhao, C. Q. Zhao, M. Li, J. S. Ren and X. G. Qu, *Anal. Chim. Acta*, 2014, **809**, 128.
20 W. L. Wei, C. Xu, L. Wu, J. S. Wang, J. S. Ren and X. G. Qu, *Sci. Rep.*, 2014, **4**, 3564.
21 Y. Q. Zhang, D. K. Ma, Y. Zhuang, X. Zhang, W. Chen, L. L. Hong, Q. X. Yan, K. Yu and S. M. Huang, *J. Mater. Chem.*, 2012, **22**, 16714.
22 D. H. Seo, A. E. Rider, S. Kumar, L. K. Randeniya and K. Ostrikov, *Carbon*, 2013, **60**, 221.
23 J. Wang, C. F. Wang and S. Chen, *Angew. Chem. Int. Ed.*, 2012, **51**, 9297.
24 S. Sahu, B. Behera, T. K. Maiti and S. Mohapatra, *Chem. Commun.*, 2012, **48**, 8835.
25 H. Huang, J. J. Lv, D. L. Zhou, N. Bao, Y. Xu, A. J. Wang and J. J. Feng, *RSC Adv.*, 2013, 3, 21691.
26 S. Liu, J. Q. Tian, L. Wang, Y. W. Zhang, X. Y. Qin and Y. L. Luo, *Adv. Mater.*, 2012, 24, 2037.
27 C. Mattevi, G. Eda, S. Agnoli, S. Miller, K. A. Mkhoyan, O. Celik, D. Mastrogiovanni, G. Granozzi, E. Garfunkel and M. Chhowalla, *Adv. Funct. Mater.*, 2009, **19**, 2577.
28 J. P. Paraknowitsch, Y. J. Zhang, B. Wienert and A. Thomas, *Chem. Commun.*, 2013, **49**, 1208.
29 K. P. Gong, F. Du, Z. H. Xia, M. Durstock and L. M. Dai, *Science*, 2009, **323**, 760.
30 J. F. Moulder, W. F. Stickle, P. E. Sobel and K. D. Bomben, *Perkin-Elmer Corporation*, Eden Prairie, MN, USA, 1992.
31 S. B. Yang, L. J. Zhi, K. Tang, X. L. Feng, J. Maier and K. Müllen, *Adv. Funct. Mater.*, 2012, **22**, 3634.
32 H. Fang, M. J. Fang, X. X. Liu, P. X. Xu and Y. F. Zhao, *Chinese J. Org. Chem.*, 2005, **25**, 466.
33 H. Peng and J. Travas-Sejdic, *Chem. Mater.*, 2009, **21**, 5563.

34 S. J. Zhu, J. H. Zhang, S. J. Tang, C. Y. Qiao, L. Wang, H. Y. Wang, X. Liu, B. Li, Y. F. Li, W. L. Yu, X. F. Wang, H. C. Sun and B. Yang, *Adv. Funct. Mater*., 2012, **22**, 4732.

35 J. Jiang, Y. He, S. Y. Li and H. Cui, *Chem. Commun.*, 2012, **48**, 9634.

36 J. Peng, W. Gao, B. K. Gupta, Z. Liu, R. Romero-Aburto, L. Ge, L. Song, L. B. Alemany, X. B. Zhan, G. H. Gao, S. A. Vithayathil, B. A. Kaipparettu, A. A. Marti, T. Hayashi, J. J. Zhu and P. M. Ajayan, *Nano Lett.*, 2012, **12**, 844.

37 H. Huang, J. J. Lv, D. L. Zhou, N. Bao, Y. Xu, A. J. Wang and J. J. Feng, *RSC Adv.*, 2013, **3**, 21691.

38 Y. Dong, N. Zhou, X. Lin, J. Lin, Y. Chi and G. Chen, *Chem. Mater.*, 2010, **22**, 5895.

39 X. Yan, B. S. Li, X. Cui, Q. S. Wei, K. Tajima and L. S. Li, *J. Phys. Chem. Lett.*, 2011, **2**, 1119.

40 H. P. Liu, T. Ye and C. D. Mao, *Angew. Chem. Int. Ed.*, 2007, **46**, 6473.

41 H. T. Li, X. D. He, Z. H. Kang, H. Huang, Y. Liu, J. L. Liu, S. Y. Lian, C. H. A. Tsang, X. B. Yang and S. T. Lee, *Angew. Chem. Int. Ed.*, 2010, **49**, 4430.

42 K. P. Loh, Q. Bao, G. Eda and M. Chhowalla, *Nat. Chem.*, 2010, **2**, 1015.

43 X. Wang, L. Cao, S. T. Yang, F. S. Lu, M. J. Meziani, L. L. Tian, K. W. Sun, M. A. Bloodgood and Y. P. Sun, *Angew. Chem. Int. Ed.*, 2010, **49**, 5310.

44 L. Bao, Z. L. Zhang, Z. Q. Tian, L. Zhang, C. Liu, Y. Lin, B. P. Qi and D. W. Pang, *Adv. Mater.*, 2011, **23**, 5801.

45 Y. Li, Y. Hu, Y. Zhao, G. Q. Shi, L. E. Deng, Y. B. Hou and L. T. Qu, *Adv. Mater.*, 2011, **23**, 776.

46 J. Shen, Y. Zhu, C. Chen, X. Yang and C. Li, *Chem. Commun.*, 2011, **47**, 2580.

47 S. N. Baker and G. A. Baker, *Angew. Chem. Int. Ed.*, 2010, **49**, 6726.

48 S. C. Ray, A. Saha, N. R. Jana and R. Sarkar, *J. Phys. Chem. C*, 2009, **113**, 18546.

49 X. H. Wang, K. G. Qu, B. L. Xu, J. S. Ren and X. G. Qu, *J. Mater. Chem.* 2011, **21**, 2445.

50 F. Chai, T. T. Wang, L. Li, H. Y. Liu, L. Y. Zhang and Z. M. Su, *Nanoscale Res. Lett.*, 2010, **5**, 1856.

51 H. Wang, Y. X. Wang, J. Y. Jin and R. H. Yang, *Anal. Chem.*, 2008, **80**, 9021.

Simple and green synthesis of nitrogen-, sulfur-, and phosphorus-co-doped carbon dots with tunable luminescence properties and sensing application†

Chunfeng Wang, Dong Sun, Kelei Zhuo,* Hucheng Zhang, and Jianji Wang*

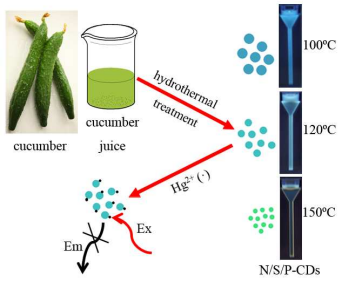

N/S/P-co-doped carbon dots with tunable luminescence properties were synthesized from cucumber juice, and used as fluorescent probe for Hg^{2+} detection.